Manifestation of external field effect in time-resolved photo-dissociation dynamics of LiF

Manifestation of external field effect in time-resolved photo-dissociation dynamics of LiF*

Meng Qing-Tian(孟庆田)[a)†] and A. J. C. Varandas[b)]

[a)] *Department of Physics, Institute of Physics and Electronics, Shandong Normal University, Jinan* 250014, *China*
[b)] *Departamento de Quimica, Universidade de Coimbra*, 3004-535 *Coimbra, Portugal*

(Received 1 February 2013; revised manuscript received 28 February 2013)

The photo-dissociation dynamics of LiF is investigated with newly constructed accurate *ab initio* potential energy curves (PECs) using the time-dependent quantum wave packet method. The oscillations and decay of the wave packet on the adiabats as a function of time are given, which can be compared with the femtosecond transition-state (FTS) spectroscopy. The photo-absorption spectra and the kinetic-energy distribution of the dissociation fragments, which can exhibit the vibration-level structure and the dispersion of the wave packet, respectively, are also obtained. The investigation shows a blue shift of the band center for the photo-absorption spectrum and multiple peaks in the kinetic-energy spectrum with increasing laser intensity, which can be attributed to external field effects. By analyzing the oscillations of the wave packet evolving on the upper adiabat, an approximate inversion scheme is devised to roughly deduce its shape.

Keywords: photo-dissociation dynamics, time-dependent wave packet method, photo-absorption spectra, external field effect

PACS: 33.80.Gj, 87.15.ag **DOI:** 10.1088/1674-1056/22/7/073303

1. Introduction

For many experimental and theoretical investigations, alkali-halide photo-dissociation has long been a prototype for studying chemical reactions on femto-second time scales.[1,2] As is well known, the ideal tool for studying the real-time dynamics of photochemical reactions is the pump–probe scheme, femtosecond transition-state spectroscopy (FTS), which has been illustrated in a number of elegant experiments by Zewail and his co-workers.[3] In that method, an initial wave packet is pumped onto an excited state by an ultra-short laser pulse and then probed with another femtosecond laser. The temporal behavior of the wave packet may then involve long time decays before the appearance of the free fragments and the corresponding oscillations of the wave packet of the dissociating molecules. Thus, the laser-induced fluorescence (LIF) signal can shed light on the period variation with delay time, which is also a function of the probe pulse frequency.

For alkali halides, photo-dissociation involves two electronic states, the ground ionic state and the lowest excited covalent one, which cross at a certain inter-nuclear distance.[4] The photo-dissociation can then occur via a transition from the ground state to the excited one, with falling apart of the molecule when it encounters the crossing point of the two involved diabatic potential energy curves (PECs). In the diabatic limit, the wave packet may then transit the point of the diabatic crossing and continue to form the products. In the adiabatic extreme, however, the wave packet can get trapped in the potential well formed by the two interacting PECs. The temporal behavior in this case will be characterized by a strong resonance. FTS can therefore be expected to provide details about the shape and coupling of the PECs. Indeed, Zewail and his coworkers obtained such relevant information for NaI by analyzing the features of FTS, and concluded that the potential well has a Morse-type shape.[3]

In the interpretation of femtosecond pump–probe experiments, the theoretical treatment based on the time-dependent wave packet method has played an important role, especially in the studies of molecular photo-fragmentation,[5,6] multi-photon ionization,[7,8] and dissociation[9–13] of molecules under external fields. Using the results of wave packet calculations of dissociation dynamics with *ab initio* electronic energies and coupling elements, Regan *et al.*[14] investigated the ultraviolet photo-dissociation of HCl in selected rovibrational states. Their predictions shared common qualitative trends with the experimental results. Among the alkali halides, NaI is possibly the most extensively investigated system, with its spin–orbit effects in photo-dissociation also being of interest for many researchers.[15–18] In a time-dependent wave packet dynamics calculation, Alekseyev *et al.*[4] determined probabilities and partial cross sections for dissociation into different fine-structure states of the iodine atom. They have shown that the inclusion of the spin–orbit coupling nearly quantitatively reproduces the observed peaks in the absorption spectra.

Lithium fluoride (LiF), a paradigmatic example of a molecule with two states that show an avoided crossing,

*Project supported by the International Cooperation Program for Excellent Lectures of 2008 by Shandong Provincial Education Department, China, the National Natural Science Foundation of China (Grant No. 11074151), and Fundação para a Ciência e a Tecnologia, Portugal.

†Corresponding author. E-mail: qtmeng@sdnu.edu.cn

has also long been the object for studying the photolysis dynamics.[19–22] Its PECs suggest that a manifestation of non-adiabatic behavior is likely to occur in the chemi-ionization process Li+F→Li^++F^-. Based on the early curves, Bandrauk *et al.*[23] investigated the multi-photon dissociation of LiF in the presence of a non-resonant external infrared laser field by solving numerically the coupled equations in a dressed molecule representation. Although the PECs used may not be accurate in today's standard, the calculations present a sketchy outline of the multi-photon absorption width. Since LiF is an ideal candidate for the above-threshold photo-dissociation, Bandrauk *et al.*[24] have also investigated the latter as well as the influence of its large dipole moment on photo-fragmentation via numerical simulations. In turn, Balakrishnan *et al.*[25] employed *ab initio* PECs and transition dipole matrix elements given by Werner and Meyer[26] to perform a wave packet study of LiF photo-dissociation, having found that extremely narrow resonances and a broad window resonance are atop a broad absorption envelope, in agreement with the stationary-state calculations. However, due to the limitations of the calculation scheme, their result can neither explain the effect of external fields on the dissociation nor deal with the inverse problem of extracting potential properties from the spectrum.

Recently, one of us[27,28] published accurate *ab initio* PECs for the Li–F ionic-covalent interaction by extrapolation to the complete basis set limit and modeled the radial non-adiabatic coupling. In comparison with other published PECs, the calculated interaction potentials show geometric and energetic attributes of unprecedented accuracy, including the region of the diabatic crossing. It will therefore be interesting to study the photo-dissociation of LiF under an external field using the newly constructed PECs. The purpose of this paper is then to present a time-dependent wave packet treatment of the photo-dissociation of LiF and provide a physically intuitive picture of the dynamics with the new *ab initio* PECs and transition dipole matrix elements. The emphasis will be on the influence of external laser fields on the dissociation properties of LiF by using a different treatment to prepare the wave packet. By analyzing the details of wave packet formation, dispersion, as well as the features of the photo-absorption and kinetic-energy spectra of the dissociation products, additional physical insight into the shape of the PECs will be given.

The paper is organized as follows. Section 2 provides a brief review of the quantum wave packet methodology for photo-dissociation. Schrödinger's equation and its solution with the scheme of wave packet propagation are then briefly described, with the method used to calculate the photo-dissociation absorption spectrum and the kinetic-energy spectrum being outlined also. Section 3 gives the results. The discussion on the effect of external laser fields on the properties of photo-dissociation and the possibility of extracting information about the PECs from the propagation of the wave packet is also presented in this section. Concluding remarks are given in Section 4.

2. Methodology

2.1. Schrödinger equation for a two-state system and its canonical solution

Consider a two-state system coupled by a laser field of frequency ω_L, i.e.,[29]

$$E(t) = E_0 f(t) \sin(\omega_L t), \tag{1}$$

where $f(t)$ is the envelope function which is commonly taken of the Gaussian form, and E_0 is the maximum field amplitude. By employing the Born–Oppenheimer approximation and ignoring the coupling of rotation with other degrees of freedom, the radial Schrödinger equation for the system assumes the form

$$\mathrm{i}\hbar \frac{\partial}{\partial t} \boldsymbol{\Psi}(R,t) = \boldsymbol{H} \boldsymbol{\Psi}(R,t), \tag{2}$$

where $\boldsymbol{H} = \boldsymbol{T} + \boldsymbol{V}$ is the system Hamiltonian, and the wave function is defined by

$$\boldsymbol{\Psi}(R,t) = \begin{pmatrix} \psi_g(R,t) \\ \psi_e(R,t) \end{pmatrix}, \tag{3}$$

where g and e label the ground and the excited states, respectively. Thus,

$$\boldsymbol{T} = -\frac{\hbar^2}{2m}\frac{\partial^2}{\partial R^2}\begin{pmatrix} 1 & 0 \\ 0 & 1 \end{pmatrix}, \quad \boldsymbol{V} = \begin{pmatrix} V_g & W_{ge} \\ W_{eg} & V_e \end{pmatrix}, \tag{4}$$

where m is the reduced mass, $V_g(R)$ and $V_e(R)$ are the diabatic potential functions (diabats) for the ground and the excited state curves, respectively, and

$$W_{ge} = W_{eg} = V_{ge} + \mu(R)E(t), \tag{5}$$

with V_{ge} being the non-adiabatic coupling and $\mu(R)$ the transition dipole moment. In Eq. (3), $\psi_g(R,t)$ and $\psi_e(R,t)$ represent the time-dependent nuclear wave functions in the lower and the upper states, respectively, which are obtained by the following wave packet propagation scheme, the split-operator technique.[30]

Consider a small time interval Δt. By using the split-operator technique, the canonical solution of Eq. (2) can be written up to the second-order approximation as

$$\boldsymbol{\Psi}(R,t_0+\Delta t) \approx [\boldsymbol{U}_{\boldsymbol{T}}^{1/2} \boldsymbol{U}_{\boldsymbol{V}}(R,t_0) \boldsymbol{U}_{\boldsymbol{T}}^{1/2}] \boldsymbol{\Psi}(R,t_0), \tag{6}$$

where $\boldsymbol{\Psi}(R,t_0)$ is the wave packet at the initial time t_0, and

$$\boldsymbol{U}_{\boldsymbol{T}} = \exp\left[-\frac{\mathrm{i}\Delta t}{\hbar}\boldsymbol{T}\right], \quad \boldsymbol{U}_{\boldsymbol{V}} = \exp\left[-\frac{\mathrm{i}\Delta t}{\hbar}\boldsymbol{V}(R,t_0)\right] \tag{7}$$

are called the kinetic- and potential-energy evolution operators, respectively. After propagating n steps, the wave function assumes the form

$$\boldsymbol{\Psi}(R,t_0+n\Delta t) \approx \left[\prod_{k=0}^{n-1} \boldsymbol{U_T U_V}(R,t_0+k\Delta t)\right] \boldsymbol{\Psi}(R,t_0). \quad (8)$$

As usual, the action of $\boldsymbol{U_V}$ is carried out in the coordinate space, and that of $\boldsymbol{U_T}$ in the momentum space, where such operators are diagonal. In the present treatment of the basis functions, the discrete variable representation (DVR) method is used,[31,32] which provides a flexible choice of basis sets and grids. Correspondingly, a fast-Fourier-transform algorithm is used to switch efficiently between the coordinate and momentum spaces following the application of each exponential operator. The exponential potential-energy part in Eq. (8) is evaluated by diagonalizing the 2×2 potential-energy matrix at each grid point in the radial coordinate R.

Now let the nuclear wave packet be denoted as $\psi_i(R,t)$ (i=g, e). The wave function at arbitrary time will assume the form $\boldsymbol{\Psi}(R,t) = (\psi_{\rm g}((R,t),\ \psi_{\rm e}((R,t))^{\rm T}$, with the population of each state being extracted from the nuclear wave packet $\psi_i(R,t)$ (i =g, e) norm[33]

$$P_i(t) = \int_{R_1}^{R_2} {\rm d}R|\psi_i(R,t)|^2, \quad (9)$$

where R_1 and R_2 define the range of inter-nuclear distances. Information associated with the wave packet $\psi_i(R,t)$ (i =g, e) can be similarly obtained. Since the field parameters influence the Hamiltonian of the system, the wave packet and the effect of external fields on the photo-dissociation process can be studied by analyzing the information obtained when varying such parameters.

2.2. Absorption potential and other photo-dissociation information

As is well known, in time-dependent wave packet calculations for scattering problems, a common difficulty is the reflection of the wave function at the borders of the numerical grid which can distort and ruin the correct dynamics.[34] A robust approach is to employ an absorbing (or optical) potential which eliminates the wave function near the grid boundary, thus eliminating the artificial boundary reflections. In this work, we use a quartic complex absorbing potential defined as[5]

$$\begin{aligned} &V_{\rm damp}(R) = 0, \quad R < R_{\rm damp}, \\ &V_{\rm damp}(R) = -{\rm i}C_{\rm damp}\left(\frac{R-R_{\rm damp}}{R_{\rm max}-R_{\rm damp}}\right)^4, \\ &R_{\rm damp} < R < R_{\rm max}, \end{aligned} \quad (10)$$

where $R_{\rm damp}$ is the point at which the damping is switched on, and $C_{\rm damp}$ is an optimized parameter giving the damping strength.

Once the wave packet at $R_{\rm damp}$ is obtained, it can be Fourier transformed from time to energy domain as

$$\psi_i(E) = \frac{1}{2\pi}\int_0^\infty \psi_i(R_{\rm damp},t)\exp(-{\rm i}Et/\hbar){\rm d}t, \quad (11)$$

then the partial cross section in channel i is extracted according to[4]

$$\sigma_i(\omega) = \frac{4\pi^3}{3c\varepsilon_0 m}k_i\omega|\psi_i(E)|^2, \quad (12)$$

with $k_i = \sqrt{2m(E-V_i(R_{\rm f}))}/\hbar$ being the wave vector in channel i, $V_i(R_{\rm f})$ the potential energy in channel i at $R = R_{\rm f}$, and ε_0 the permittivity of free space. So the total photo-absorption spectrum as a function of the photon energy $\hbar\omega$ is then given by the sum of the partial cross sections in Eq. (12)

$$\sigma_{\rm tot}(\omega) = \sum_i \sigma_i(\omega). \quad (13)$$

Regarding the dissociation probability, it can be calculated for a given channel from the probability flux of the wave function at the nuclear separation $R_{\rm damp}$

$$J_i(t) = \frac{\hbar}{m}{\rm Im}\left[\psi_i^*(R,t)\frac{\partial\psi_i(R,t)}{\partial R}\right]_{R=R_{\rm damp}}, \quad (14)$$

with the time-integrated flux yielding the dissociation probability. If we write the outgoing wave packet in terms of a real amplitude A and a real phase ϕ

$$\psi_i(R,t) = A_i(R,t)\exp[{\rm i}\phi_i(R,t)], \quad (15)$$

then the current density can be written as

$$J_i(R,t) = \frac{|A_i(R,t)|^2}{m}\nabla\phi_i(R,t), \quad (16)$$

from which we can obtain

$$\nabla\phi_i(R,t) = \frac{J_i(R,t)m}{|A_i(R,t)|^2}. \quad (17)$$

To obtain the nuclear momentum distribution of dissociation, we numerically calculate the gradient of $\phi_i(R,t)$ at $R_{\rm damp}$

$$p_i(R,t) = \nabla\phi_i(R,t) = \frac{J_i(R,t)m}{|A_i(R,t)|^2}, \quad (18)$$

where equation (17) has been used. According to the definition of the flux density, the probability for finding the number of 'events' (ΔN) with momenta p within a small interval Δp around a momentum p_j is given by

$$\begin{aligned} \Delta N(p_j) &= \Delta p\int_0^\infty {\rm d}tJ_i(R_{\rm damp},t) \\ &\times\begin{cases} 1, & \text{for } p\in[p_j-\Delta p/2, p_j+\Delta p/2], \\ 0, & \text{else.} \end{cases} \end{aligned} \quad (19)$$

If $J_i(R_{\rm damp},t)$ has dominant contributions only for a sufficiently large t, then the momentum distribution can be expressed as[35]

$$\left.\frac{{\rm d}N}{{\rm d}p}\right|_{p'} = \frac{J_i(R_{\rm damp},t(p'))}{\left|\frac{{\rm d}p}{{\rm d}t}(t(p'))\right|}, \quad (20)$$

where p' is the momentum at which the derivative is calculated. Correspondingly, the kinetic-energy spectrum can be written as

$$\left.\frac{\mathrm{d}N}{\mathrm{d}E}\right|_{T'} = \sqrt{\frac{2m}{T'}}\left.\frac{\mathrm{d}N}{\mathrm{d}p}\right|_{P'=\sqrt{2\mu T'}}. \tag{21}$$

The dissociation yield of fragments, D, can finally be obtained from the following integration along the nuclear flux direction at R_{damp}:

$$D(t) = \int_0^t \mathrm{d}t' J_i(R_{\mathrm{damp}}, t'). \tag{22}$$

3. Results and discussion

For LiF, there is little non-Born–Oppenheimer mixing of the singlet states X $^1\Sigma^+$ and B $^1\Sigma^+$ with the triplet states. The extent of photo-excitation to the B state, and hence the total photo-dissociation cross section, will therefore be little affected by such states. Thus, the two-state model based only on the PECs of the X and B singlet states should be reliable for dealing with the photo-dissociation process. Accordingly, the total photo-dissociation cross section will be sensitive only to the shape of the B state and the magnitude and shape of the X–B transition dipole. Figures 1 and 2 show the diabats and the transition dipole moment utilized in the present work as a function of the bond distance, respectively.[27,28] Clearly, they exhibit the varying character of the electronic configurations from ionic to covalent as the point $R_{\mathrm{c}} = 13.5a_0$ is crossed, where a_0 is the Bohr radius.

With the PECs and the transition dipole moment function, the bound state wave function can be computed using the Fourier-grid Hamiltonian method. Accordingly, the initial wave packet

$$\boldsymbol{\Psi}(R,0) = \begin{pmatrix} \psi_{\mathrm{g}}(R,0) \\ \psi_{\mathrm{e}}(R,0) \end{pmatrix} = \begin{pmatrix} \psi_{\mathrm{g}}(R,0) \\ 0 \end{pmatrix} \tag{23}$$

is accurately known, and the wave packet can be obtained at any time via the wave-packet propagation scheme. Details concerning the latter are reported in Table 1.

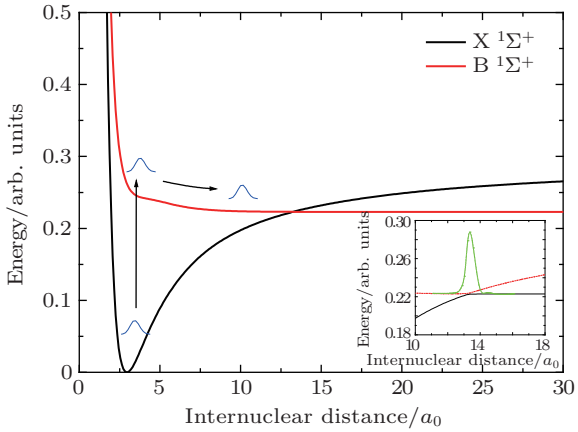

Fig. 1. (color online) Diabatic (solid line) and adiabatic (dashed line in the insert, with the upper line being the diabatic coupling term) PECs for LiF.[27]

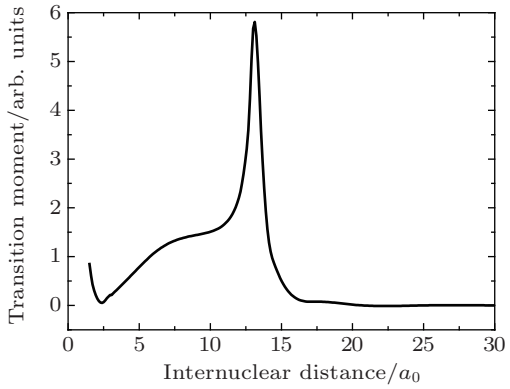

Fig. 2. Transition dipole moment as a function of inter-nuclear distance.[27]

Table 1. Numerical parameters used to perform the time-dependent wave-packet calculation.

Time and space		Laser pulse		Absorbing potential	
Range of grid/a_0	1.5–50	Wavelength/nm	350–365	R_{damp}/a_0	48
Number of grid points	1024	Intensity/W·cm^{-2}	8×10^{10}–8×10^{14}	R_{damp}/a_0	50
Number of time steps	8192	Half-width/fs	50	C_{damp}	20
Time step/fs	0.2441				

3.1. Evolution of the wave packet on the upper adiabat

The spatial spread of the wave packet has important consequences on the computed spectrum, and carries the signature of the dissociation dynamics on the excited-state potential. For this reason, we provide a detailed analysis of the spatial evolution of the wave packet following the initial excitation, and attribute details of the photo-absorption spectrum to specific aspects of the wave packet motion.

The initial excitation within the ionic state covers a broad range of energies, spanning both bound vibrational states and the region between the dissociation thresholds. Because the wave packet is not an eigenstate of the coupled Hamiltonian in Eq. (2), it disperses and builds up amplitude in the covalent state during the propagation. Figure 3 shows clearly the time changing of the wave packet amplitude, which is calculated at a reference inter-nuclear distance of $R_{\mathrm{ref}} = 10a_0$ or so. As is clearly shown, after the wave packet is pumped to the covalent state, it reaches the point of R_{ref} at about 160 fs, moving forward continuously along the potential well formed by the interacting adiabats. Then at about 735 fs, it moves backwards

after arriving at the right-hand-side turning point. Since it encounters the interaction region from the left, part of it transmits across this region to the other PEC, with the decay of its amplitude inevitably emerging. At about 905 fs, the wave packet moves forwards again after hitting the left-hand-side turning point, hence completing the first period (T) of oscillation in the potential well of the upper adiabat. In the next period, one can expect some dispersion of the wave packet. Note that the location of the maximum amplitude may differ with the choice of $R_{\rm ref}$ for a given wavelength and intensity of the laser pulse, but the oscillation period T and the pattern of motion described above remain the same.

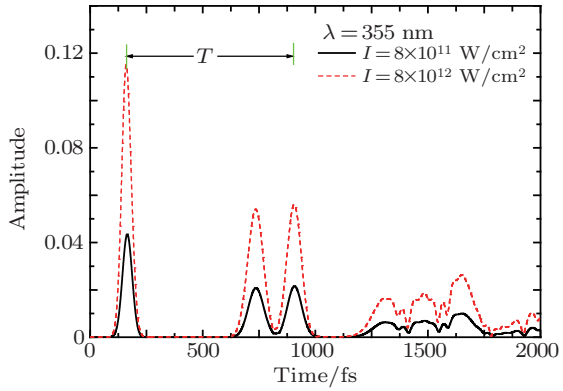

Fig. 3. (color online) Variation of the amplitude of the wave packet evolving on the upper state as a function of time delay.

One very interesting feature in Fig. 3 is that the position of the maximum (as expected, larger in amplitude) has a slight left shift when the laser intensity changes from 8×10^{11} W/cm^2 to 8×10^{12} W/cm^2, and a more obvious dispersion of the wave packet takes place. Since the number of molecules pumped to the excited state is proportional to the laser intensity, it is easy to understand the increase of amplitude with intensity. Regarding the left shift and the dispersion of the wave packet, they are often attributed to the anharmonicity of the potential. In fact, as shown in Eqs. (1) and (5), the increase in laser intensity enhances the coupling strength of the two PECs and, as a result, the shape of the adiabats is modified, leading to a change of anharmonicity. Such an external field effect has been described by many theoreticians.[7,36]

3.2. Photo-dissociation cross section

In the time-dependent quantum-mechanical formalism, the photo-absorption spectrum is generically determined by the autocorrelation function, which is defined as the projection of the propagated wave function onto the localized initial-state wave-packet at each time step.[26] Since the excited-state covalent PEC is modified by the field–molecule interaction, the absorption spectrum will exhibit the influence of the interaction. However, because the initial state is just a product of the rovibrational wave function for the ground-state potential and the transition dipole moment between the ground and the excited electronic states, and what is more, in the propagation of wave packet with the split-operator scheme, the general method will be unable to give the effect of the external field on the photo-dissociation due to the field coupling not being included in the potential evolution operator. To fill up this deficiency, in the present work we use an explicit field coupling as the interaction potential (Eqs. (4) and (5)), and hence the evolution of the wave packet now naturally contains information relevant to the external field (Eqs. (6)–(8)). Correspondingly, eqs. (12) and (13) are utilized to calculate partial and total cross sections instead of the Fourier transform of the autocorrelation function.[26] Alekseyev *et al.*[4] have verified that for a given time-dependent wave function, the two methods give the same total cross section. For convenience, the total propagation time is here taken as 2000 fs, which can give the spectrum with reasonable resonance positions and profiles compared with the results obtained from the time-independent quantum-mechanical calculation of Cornett *et al.*[37] Figure 4 shows the photo-absorption cross section at a laser wavelength of $\lambda = 355$ nm for different laser intensities. One common feature of these figures is that in each absorption spectrum there is a broad envelope, which is superimposed with a series of extremely narrow resonances separated by broad window resonances that recur periodically. This phenomenon has to do with the oscillations of the wave packet trapped in the well of the upper adiabat.

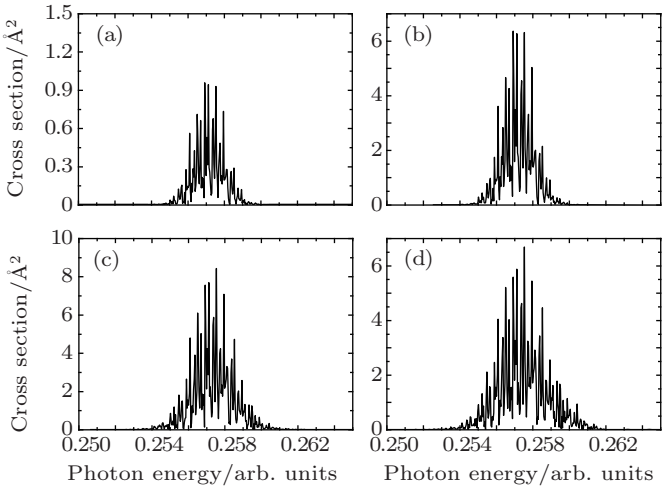

Fig. 4. Photo-dissociation cross section at wavelength of $\lambda = 355$ nm and different laser intensities ((a) 8×10^{11} W/cm^2, (b) 8×10^{12} W/cm^2, (c) 5×10^{13} W/cm^2, (d) 1×10^{14} W/cm^2).

As one could expect, the photon energy corresponding to the highest peak is the most probable energy with which the photon can be absorbed. From Fig. 4, one can also observe that the bandwidth increases with increasing laser intensity, while the band center displays a slight blue shift. From the above analysis, one may expect that the coupling of the two electronic states by the external field may change the separation of

the two PECs in the Frank–Condon region, which may explain the blue shift of the band center. Certainly, with increasing laser intensity, the photons with other frequencies and small absorption probabilities now find enhanced probabilities of being absorbed in the photo-dissociation process, which may explain the bandwidth increase noted above. Another feature in Fig. 4 refers to a series of broad window resonances in each spectrum, which, we believe, arises from the periodic oscillations and the vibrational components of the wave packet in the potential well of the upper adiabat. To test this conjecture, figure 5 shows the vibrational projection of the wave packet (at time delay 720 fs and laser intensity 8×10^{12} W/cm^2) oscillating in the upper adiabat. Obviously, the vibrational level structure of the oscillating wave packet shows a profile similar to the one in Fig. 4(b). With increasing laser intensity, the dispersion of the wave packet leads to maximum projection on the vibrational states of the adiabatic potential well that have a larger quantum number. In other words, the photons taking part in the resonance absorption are the more energetic ones in this case.

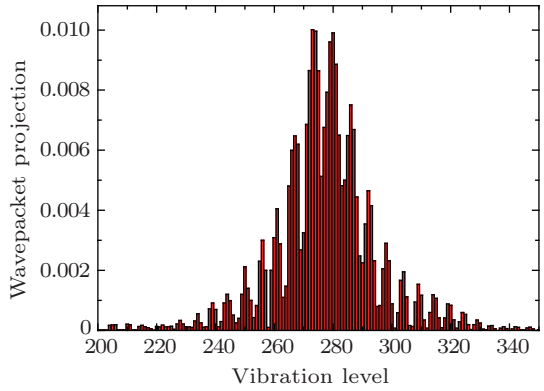

Fig. 5. (color online) Projection of wave packet on different vibrational levels in the adiabatic potential well.

3.3. Dissociation kinetic-energy spectra

The external field effect in photo-dissociation is also visible from the dissociation kinetic-energy spectrum. Figure 6 shows the kinetic energy of the dissociative fragments for laser intensities varying from 8×10^{11} W/cm^2 to 1×10^{14} W/cm^2. At low intensities (say 8×10^{11} W/cm^2 in Fig. 6(a)), the dissociation fragments have a small kinetic energy (say 0.06 eV). With an increase of the laser intensity to 8×10^{12} W/cm^2, the kinetic energy of the fragments would increase to 0.07 eV (Fig. 6(b)), but the dissociation probability drastically decreases. An increase of the laser intensity will then lead to recurrences of the fragment energy and the dissociation probability even larger than that displayed in Figs. 6(a) and 6(c). This pattern for the dissociation probability to change with the laser intensity is consistent with the observation reported by Feuerstein *et al.*[5] in the investigations of H_2^+ fragmentation under laser pulses. The simulations show that such a change of the fragment energy with the laser intensity has to do with the modification of the PEC by the external field. Just as discussed above, the modified PEC will distort the wave packet evolving on the upper adiabatic potential well, with the distortion increasing with increasing laser intensity. Figure 7 shows the evolution of the wave packet in the potential well of the upper adiabat over a time range from 1200 fs to 2000 fs and at the laser intensity of 1×10^{14} W/cm^2. The distortion of the wave packet is clearly visible. In addition, a comparison of Fig. 7 with Fig. 6(d) can give a hint for the origin of peaks appearing in the kinetic-energy spectrum. In the evolution of the wave packet in the dissociative channel, the dispersion of the wave packet gives rise to four peaks denoted by 1, 2, 3, and 4 in Fig. 7, which arrive at the same inter-nuclear distance but at different times. Such a phenomenon corresponds to the appearance of four peaks in Fig. 6(d), also denoted by 1, 2, 3, and 4 and located at increasing kinetic energies.

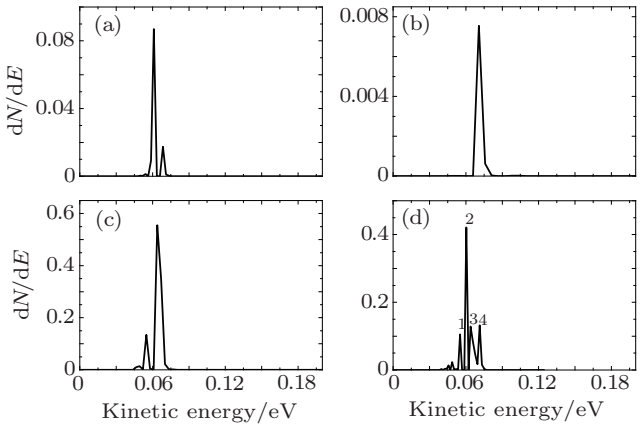

Fig. 6. Kinetic-energy distributions of dissociation fragments for laser intensities of (a) 8×10^{11} W/cm^2, (b) 8×10^{12} W/cm^2, (c) 5×10^{13} W/cm^2, and (d) 1×10^{14} W/cm^2.

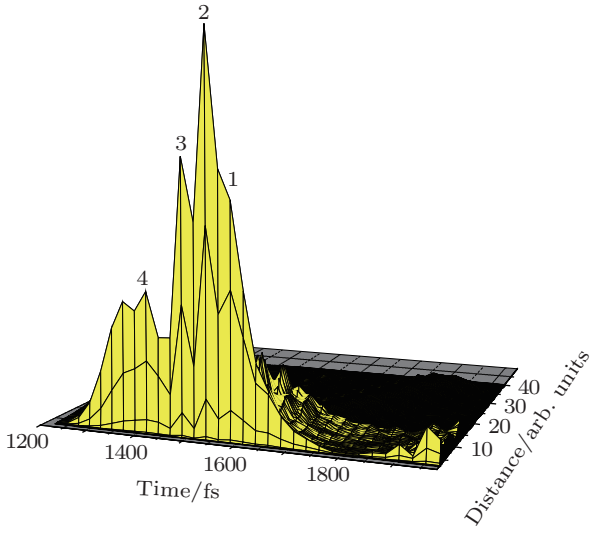

Fig. 7. (color online) Evolution of wave packet with time and space in dissociation channel. The marks 1–4 correspond to the ones in Fig. 6(d).

3.4. Deducing information about the potential from FTS

One interesting thing for experimentalists and theorists is to get information about the PECs from FTS, a technique to

detect the real-time dynamics of wave packet resonances. In fact, a similar result to FTS has been given in Fig. 3, which vividly shows the oscillation of the wave packet on the adiabatic excited state. From this figure, one can deduce that the oscillation period of the wave packet trapped in the shallow well of the adiabatic potential is about 745 fs. Suppose now that the shape of the shallow well can be described by an anharmonic oscillator (AO) of the Morse-type. The vibrational energy levels in this case are given by the expression[38]

$$E_n = h\nu_0\left(n+\frac{1}{2}\right) - h\chi\nu_0\left(n+\frac{1}{2}\right)^2, \tag{24}$$

where n is the quantum number, ν_0 is the oscillator harmonic frequency, and χ is the anharmonicity parameter $(0 \leq \chi \leq 1)$ which can be defined by $\chi = h\nu_0/(4D)$, with D being the potential well-depth. According to Eq. (24), the energy spacing, and thus the wave packet frequency, should decrease for the AO with increasing energy. In the classical limit, the relationship between the wave packet oscillation frequency and the energy is given by[3]

$$\nu^2_{\text{packet}} = \nu_0^2 - 4\chi\nu_0(\nu_{\text{pump}} - \nu_{\text{diss}}), \tag{25}$$

where ν_{diss} is the frequency corresponding to the dissociation energy. To extract the period T of the wave packet oscillation in the potential well, the pump laser wavelength varies from 350 nm to 365 nm in our calculations. Figure 8 displays the fitted results, which are obviously well described by the above simple relationship, giving a slope of 1.60×10^{10} s^{-1}. This slope corresponds to the anharmonicity parameter $\chi = 0.35$. Clearly, only a limited range of energies (350–365 nm) of the adiabatic curve have been tested in these preliminary calculations. Extending it to other parts of the potential curve requires further information.

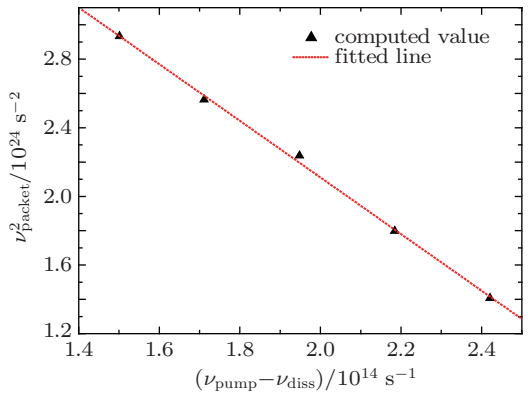

Fig. 8. (color online) Square of the frequency of the wave packet oscillation as a function of the laser pump frequency minus the frequency corresponding to the dissociation energy.

4. Conclusion

In this paper, we have investigated the photo-dissociation dynamics of LiF using time-dependent wave packet quantum dynamics with accurate *ab initio* PECs and transition dipole moments. The emphasis is on the influence of external fields on the oscillation of the wave packet in the upper adiabat, photo-absorption spectra, as well as dissociation kinetic-energy distributions. Many interesting phenomena occurring in the photo-dissociation process are related to the avoided crossing of the ground and excited states. The simulations have shown that due to the avoided crossing the wave packet oscillates in the adiabatic potential well, with the dispersion of the wave packet in the ionic channel originating from both the modified PECs by the laser-molecule interaction and the avoided crossing. For increasing laser intensity, the band center of the total cross section has shown a trend towards blue shift, with the peaks appearing in the dissociation kinetic-energy spectra being attributed to the dispersion of wave-packet evolving in the adiabatic PECs. By analyzing the variation of the amplitude of the wave packet with delay time, we are able to inquire about the shape of the potential well using a simple inversion scheme. It should be noted that the laser intensity 10^{11}–10^{14} W/cm^2 used in this work is not strong, so equation (12) for calculating the partial cross section is a suitable choice. For the calculation in intense laser fields, the reader is referred to Ref. [39]. Of course, no spin–orbit coupling has been taken into consideration in this work. We are looking forward to experimental studies on the photo-dissociation of LiF that may allow a comparison between the theoretical predictions and the experimental observations.

References

[1] Rose T S, Rosker M J and Zewail A H 1988 *J. Chem. Phys.* **88** 6672
[2] Cong P, Mokhtari A and Zewail A H 1990 *Chem. Phys. Lett.* **172** 109
[3] Rosker M J, Rose T S and Zewail A H 1988 *Chem. Phys. Lett.* **146** 175
[4] Alekseyev A B, Liebermann H P and Buerker R J 2000 *J. Chem. Phys.* **113** 1514
[5] Feuerstein B and Thumm U 2003 *Phys. Rev. A* **67** 043405
[6] Li X, Yang H and Ma R 2004 *Chin. Phys.* **13** 1564
[7] Meng Q T, Yang G H, Sun H L, Han K L and Lou N Q 2003 *Phys. Rev. A* **67** 063202
[8] Chen J X and Gong Q H 2005 *Chin. Phys.* **14** 1960
[9] Yue D G, Zheng X Y, Liu H and Meng Q T 2009 *Chin. Phys. B* **18** 1479
[10] Clark A P, Brouard M, Quadrini F and Vallance C 2006 *Phys. Chem. Chem. Phys.* **8** 5591
[11] Su Q Z, Yu J, Yuan K J and Cong S L 2012 *J. Theor. Comp. Chem.* **11** 709
[12] He H X, Lu R F, Zhang P Y, Han K L and He G Z 2012 *J. Chem. Phys.* **136** 024311
[13] Cong S L, Wang S M and Yuan K J 2005 *Chin. Phys. Lett.* **22** 2534
[14] Regan P M, Ascenzi D and Brown A 2000 *J. Chem. Phys.* **112** 10259
[15] Waldeck J R, Shapiro M and Bersohn R 1993 *J. Chem. Phys.* **99** 5924
[16] Martinez T J and Levine R D 1996 *Chem. Phys. Lett.* **259** 252
[17] Peslherbe G H, Bianco R, Hynes J T and Ladanyi B M 1997 *J. Chem. Soc. Faraday Trans.* **93** 977
[18] Baba M, Kokita T, Kasahara S and Kato H 1999 *J. Chem. Phys.* **111** 9574
[19] Werner H J and Meyer W 1981 *J. Chem. Phys.* **74** 5802
[20] Nakamura H and Truhlar D G 2002 *J. Chem. Phys.* **117** 5576
[21] Chattopadhyay S, Chaudhuri R K and Mahapatra U S 2008 *J. Chem. Phys.* **129** 244108
[22] Kahn L R, Hay P J and Shavitt I 1974 *J. Chem. Phys.* **61** 3530

[23] Bandrauk A D and Gauthier J M 1989 *J. Phys. Chem.* **93** 7552
[24] Bandrauk A D and Gauthier J M 1990 *J. Opt. Soc. Am. B* **7** 1420
[25] Balakrishnan N, Esry B D and Sadeghpour H R 1999 *Phys. Rev. A* **60** 1407
[26] Werner H J and Meyer W 1981 *J. Chem. Phys.* **74** 5802
[27] Varandas A J C 2009 *J. Chem. Phys.* **131** 124128
[28] Varandas A J C 2011 *J. Chem. Phys.* **135** 119902
[29] Meng Q T, Liu X G, Zhang Q G and Han K L 2005 *Chem. Phys.* **316** 93
[30] Feit M D, Fleck J A and Steiger A 1982 *J. Comput. Phys.* **47** 412
[31] Light J C, Hamilton I P and Lill J V 1985 *J. Chem. Phys.* **82** 1400
[32] Sharafeddin O and Zhang J Z H 1993 *Chem. Phys. Lett.* **204** 190
[33] Wang J, Zhao J, Xu Y, Meng Q T and Liu W K 2010 *Chin. Phys. B* **19** 123301
[34] Neuhasuer D and Baer M 1989 *J. Chem. Phys.* **90** 4351
[35] Fererstein B and Thumm U 2003 *J. Phys. B* **36** 707
[36] Trump C, Rottke H and Wittmann M 2000 *Phys. Rev. A* **62** 063402
[37] Cornett S T, Sadeghpour H R and Cavagnero M J 1999 *Phys. Rev. Lett.* **82** 2488
[38] Grado-Caffaro M A and Grado-Caffaro M 2010 *Appl. Phys. B* **99** 753
[39] Shapiro M and Bony H 1985 *J. Chem. Phys.* **83** 1588